Published in final edited form as:
Ann Thorac Surg. 2013 March ; 95(3): 825–830. doi:10.1016/j.athoracsur.2012.11.039.

In-Vitro Mitral Valve Simulator Mimics Systolic Valvular Function of Chronic Ischemic Mitral Regurgitation Ovine Model

Andrew W. Siefert, M.S.[1], **Jean Pierre Rabbah, B.S.**[1], **Kevin J. Koomalsingh, M.D.**[2], **Steven A. Touchton Jr., B.S.**[1], **Neelakantan Saikrishnan, Ph.D.**[1], **Jeremy R. McGarvey, M.D.**[2], **Robert C. Gorman, M.D.**[2], **Joseph H. Gorman III, M.D.**[2], and **Ajit P. Yoganathan, Ph.D.**[1]

[1]The Wallace H. Coulter Department of Biomedical Engineering, Georgia Institute of Technology and Emory University

[2]The Perelman School of Medicine, University of Pennsylvania

Abstract

Background—This study was undertaken to evaluate an *in vitro* mitral valve simulator's ability to mimic the systolic leaflet coaptation, regurgitation, and leaflet mechanics of a healthy and chronic ischemic mitral regurgitation (IMR) ovine model.

Methods—Mitral valve size and geometry of both healthy and chronic IMR ovine animals was used to recreate systolic mitral valve function *in vitro*. A2-P2 coaptation length, coaptation depth, tenting area, anterior leaflet strain, and mitral regurgitation were compared between the animal groups and valves simulated in the bench-top model.

Results—For the control conditions, no differences were observed between the healthy animals and simulator in coaptation length (p=.681), coaptation depth (p=.559), tenting area (p=.199), and anterior leaflet strain in the radial (p=.230) and circumferential (p=.364) directions. For the chronic IMR conditions, no differences were observed between the models in coaptation length (p=.596), coaptation depth (p=.621), tenting area (p=.879), and anterior leaflet strain in the radial (p=.151) and circumferential (p=.586) directions. Mitral regurgitation was similar between IMR models with an asymmetric jet originating from the tethered A3-P3 leaflets.

Conclusion—This study is the first to demonstrate the effectiveness of an *in vitro* simulator to emulate the systolic valvular function and mechanics of a healthy and chronic IMR ovine model. The *in vitro* IMR model provides the capability to recreate intermediary and exacerbated levels of annular and subvalvular distortion at which IMR repairs can be simulated. This system provides a realistic and controllable test platform for the development and evaluation of current and future IMR repairs.

Keywords

in-vitro studies; mitral valve; ischemic heart disease

Correspondence: Ajit P. Yoganathan,313 Ferst Dr., Atlanta, GA 30332,Ph. (404)894-2849, Fax.(404) 894-4243, ajit.yoganathan@bme.gatech.edu.

Introduction

In the past decade, the surgical repair of ischemic mitral regurgitation (IMR) has been improved with the implantation of an undersized complete (semi)rigid annuloplasty ring and coronary revascularization [1,2]. While undersized annuloplasty (UA) is effective in the majority of cases, approximately 10-15% of patients suffer from postoperative left ventricular (LV) dilatation with recurrent severe mitral regurgitation (MR) [3,4]. These patients often present with a severely distended LV whose geometric papillary muscle distortions impede the ability of UA to sustain coaptation. Though the rates of recurrent MR have been reduced, several issues impede the ability to optimally treat this subset of patients [5].

A primary issue relates to identifying patients who will benefit from isolated UA [5]. While ventricular and leaflet-based measures have demonstrated significant correlations with patient outcomes, no metrics directly quantify the geometric papillary muscle (PM) distortions that give allowance or impede the compensatory effects of UA [6-9]. A secondary issue is the need to understand the geometric mechanisms and limits of IMR repairs to improve and assess their suitability for maintaining coaptation with severe or progressive PM displacement. Assessing these issues will aid in identifying patients who may benefit from a given treatment while additionally contributing to the improvement and individualization of treatment modalities [5].

One route towards assessing these clinical issues is through the use of *in vitro* mitral valve (MV) simulators. These simulators provide the unique advantage of isolating the effect of the relative PM geometry on valvular function, which in humans can be difficult to clinically assess. Moreover, *in vitro* models provide the versatility to simulate varying degrees of disease, multiple repairs, and simultaneous measures of MV mechanics that combined can be unfeasible in animal models. Despite these advantages, no bench models have been comprehensively assessed for their ability to emulate *in vivo* valve function [10-12]. Evaluating this comparison will provide a realistic and controllable test platform for the *in vitro* development and evaluation of IMR repairs. To this end, the aim of this study is to assess a MV simulator's ability to mimic the systolic leaflet coaptation, MR characteristics, and leaflet mechanics of healthy and chronic IMR ovine models.

Material and Methods

Chronic IMR Ovine Model

The animals used in this work received care in compliance with the protocols approved by the Institutional Animal Care and Use Committee at the University of Pennsylvania in accordance with the guidelines for humane care (National Institutes of Health Publication 85-23, revised 1996).

Six Dorsett Hybrid sheep received a posterior basal LV infarct to induce progressive chronic IMR. This model has been extensively studied and precisely mimics an inferior LV infarction described in humans [1-3,13]. Through a sterile left lateral thoracotomy, snares were placed to permanently occlude the proximal second and third obtuse marginal branches of the circumflex coronary artery. Following infarction, the thoracotomy was closed and IMR allowed to progress for an 8-week period prior to evaluating *in vivo* experimental endpoints.

Ovine Protocol

Control (N=6) and chronic IMR ovine subjects (N=6) were intubated, anesthetized and ventilated with isofluorane and oxygen. Surface electrocardiogram and arterial blood

pressure were monitored. A right thoracotomy was performed. Upon the heart's exposure, epicardial Doppler echocardiography images were obtained to evaluate MR (Phillips IE33 Matrix, Phillips, Amsterdam, Netherlands). MR was graded on a 0 to 4+ scale, where 0 represented no MR and 4+ represented severe MR with reversal of pulmonary vein flow.

Using published techniques, 2 mm hemispherical piezoelectric transducers (Sonometrics, London, Ontario) were localized to the mitral annulus (N=12) and A2 anterior mitral leaflet (N=5) and connected to a Series 5001 Digital Sonomicrometer (Sonometrics, London,Ontario) (Figure 1) [13]. For this study, sonomicrometry crystals were not localized to each PM tip. The ability to accurately place transducers on the PM tips can be difficult, and from our experience, PM crystals are more prone to failure. For these reasons, we utilized a historic data set that was successful in capturing the PM positions throughout the cardiac cycle [13]. After weaning each subject from cardiopulmonary bypass, a high-fidelity pressure transducer (±1mmHg) (SPR-3505; Millar Instruments, Houston, TX) was passed percutaneously into the LV through the femoral artery for continuous measurement of left ventricular pressure (LVP). Surface electrocardiogram, LVP, and arterial pressure (Hewlett-Packard 78534C monitor; Hewlett-Packard Inc, Santa Clara, CA) were monitored.

Upon establishing baseline hemodynamics (100 mmHg peak LVP; 3.3 L/min cardiac output), the three-dimensional coordinates (resolution of ±0.024 mm) of each sonometric transducer were recorded at 200 Hz with simultaneous measurements of LVP. Following experimental completion, animals were euthanized with 1 g thiopental and 80 mEq KCl. Hearts were removed and the LV opened through the interventricular septum to quantify the infarct size as a percentage of the LV [14].

In-Vitro Simulator

In vitro simulation was conducted in the extensively studied Georgia Tech left heart simulator (GTLHS) (Figure 2) [12,15-19]. This closed-loop simulator allows for precise control of annular and subvalvular MV geometry at physiological left heart hemodynamics. Excised ovine MVs are sutured to an adjustable annulus built to mimic the same size and shape measured in our healthy and chronic IMR animals (table 1). The annulus could asymmetrically dilate from a 6.5 cm^2 D-shaped orifice to 10.5 cm^2. The shape of the dilated annulus was constructed based on the posteromedially dilated annular geometries in our IMR animals. PM positions were controlled by two mechanically adjustable positioning rods capable of achieving positions in the apical, lateral, and posterior directions at a resolution of ±0.25 mm. Transmitral flow was measured using an electromagnetic probe (Carolina Medical Electronics, FM501D, East Bend, NC) mounted upstream of the atrium. Transmitral pressure was monitored with transducers mounted in the atrium and ventricle (Validyne DC-40, Northridge, CA).

Dual Camera Stereo-Photogrammetry

Dual camera stereo-photogrammetry has been successfully used in previous studies to measure MV leaflet and chordal strains *in vitro* [15,16]. In this method, tissue dye (Thermo Scientific, Waltham, MA) is used to mark the A2 cusp with a 3×3 dot array. During experimentation, two synchronized high-speed cameras image the marker array throughout the cardiac cycle at 500 Hz. From the recorded images, direct linear transformation was used to calculate the 3D coordinates of each marker [15,16]. These coordinates were subsequently used to calculate the strain for the dye-marked region of the anterior leaflet.

In-Vitro Protocol

Fresh ovine hearts were obtained and MVs excised (N=6) preserving their annular and subvalvular anatomy. MVs with an anterior leaflet height of 18-19 mm (as measured in our

ovine animals (Table 1)), type I or II PMs, and with all leaflet chordae inserting directly into each PM were selected for experimentation. Selected MVs were sutured to the simulator's annulus using a Ford interlocking stitch. For control conditions, the annulus was set to an area of 6.5 cm^2 and annular height to commissural width ratio of 15% as measured *in vivo* (Table 1). During valve suturing, care was taken to place each suture just above the valve's natural hinge and not through the leaflet tissue. Additionally, normal annular-leaflet geometric relationships were respected - anterior leaflet occupying $1/3^{rd}$ of annular circumference and commissures aligned in the 2 and 10 o'clock positions.

After annular suturing, each PM was attached to the PM control rods. Each PM was carefully positioned and fine-tuned to establish the control MV geometry as previously described [19]. Transmitral ovine pulsatile conditions were simulated (Cardiac Output 3.3 L/min, 120 beats/min, 100 mmHg transmitral pressure). Mitral coaptation was then inspected via echocardiography such that the anterior leaflet spanned approximately $2/3^{rds}$ of the A2-P2 diameter and the coaptation length was approximately 4-5 mm as measured in our healthy animals (Table 2). If the control valve geometry conditions were successfully achieved, transmitral hemodynamics, 3D echocardiography (Philips ie-33), and dual camera high-speed images of the valve were acquired.

To simulate a chronic IMR MV geometry, the valve annulus was flattened and asymmetrically dilated per the mean valvular distortions measured in our chronic IMR animals (Table 1). The PMs were adjusted per the displacements observed between an identical healthy and chronic IMR model [13]. Based on this data, the posteromedial PM was displaced 4 mm laterally, 6 mm posteriorly, and 2 basally. While the anterolateral PM was displaced 2 mm laterally, 1 mm anteriorly, and 1.5 mm apically. After the displacement of each PM, transvalvular hemodynamics was established and experimental end-points recorded.

Data and Statistical Analysis

Sonomicrometry and tissue dye coordinates acquired in both the animal and bench experiments were used to compute the anterior leaflet strain. Using a custom MATLAB program (Mathworks, Natick, MA), biquintic finite element interpolation was used to fit a surface to the recorded 3D marker coordinates [15,16,20]. Generated surfaces were used to determine the radial and circumferential strains and strain rates endured by the anterior leaflet [15]. Similar to previous studies, the referential leaflet strain configuration corresponded with the minimum LVP. All *in vitro* hemodynamic data was processed offline within a custom Matlab program and averaged over 10 consecutive cardiac cycles. *In vitro* regurgitation fractions were calculated as the total retrograde volume divided by the stroke volume. Echocardiography data were analyzed using Phillips QLab (v.7.0; Philips Healthcare; Andover, MA). To compare between animal groups and simulated conditions, a non-parametric Mann-Whitney U test was used. *In vitro* comparisons made between the control and chronic IMR conditions were completed with a Wilcoxon Signed Rank test. All statistical analyses were completed using SPSS 20 (IBM, Armonk, NY). End points are expressed as a mean ±1 standard deviation.

Results

Animal Characteristics

Baseline characteristics of the control and chronic IMR animals are presented in Table 1. Both animal groups exhibited similar weights, heart rate, peak LVP, and anterior leaflet heights. Similar to previous studies, the chronic IMR animals exhibited a reduced rate

change of LVP during isovolumetric contraction (d(LVP)/dt) and mitral annular area increase of approximately 60% as modeled within the *in vitro* simulator [13].

The simulation of the chronic IMR valve geometry was a direct function of the annular perturbations measured in our animals and the relative PM displacements determined from previously data [13]. From this data, the posteromedial PM was observed to have a mean relative displacement of 7.25 mm laterally, 10.05 mm posteriorly, and 1.75 mm basally; while the anterolateral PM exhibited a mean relative displacement of 4.04 mm laterally, 1.28 mm anteriorly, and 3 mm apically. These relative displacements were similar to those observed previously by Miller and colleagues [21]. In pilot studies, the use of theses absolute displacements resulted in PM-chordal tearing. We believe this tearing was a consequence of using post-mortem tissue whereas *in vivo* the MV is distended over a greater period of time (8 weeks) and has exhibited the capacity to actively remodel [22,23]. For these reasons, intermediary levels of these displacements were utilized (See Methods Section).

Comparison of Coaptation

Leaflet coaptation across the A2-P2 annular diameter was evaluated for coaptation length, coaptation depth, and tenting area. Measured values within each animal group were compared to those measured within the simulated conditions. For the control conditions, no significant differences were observed between the healthy animals and MV simulator in coaptation length (p=.681), coaptation depth (p=.559), and tenting area (p=.199) (table 2). Similarly for the chronic IMR conditions, no differences were observed between models in coaptation length (p=.596), coaptation depth (p=.621), and tenting area (p=.879). While not reaching statistical significance, coaptation length was consistently lower in the simulated conditions as verified by the comparatively greater coaptation depth.

To demonstrate changes in coaptation within the GTLHS, each measure of coaptation was compared between the simulated control and chronic IMR conditions. Results revealed the coaptation length to significantly decrease from the control to chronic IMR condition (p=.027) across the A2-P2 annular diameter. Additionally, coaptation depth (p=.046) and tenting area (p=.028) were observed to significantly increase with simulated chronic IMR (table 2)

Comparison of Mitral Regurgitation

Mitral regurgitation was assessed between the chronic IMR animals and simulated conditions. Within the animal group, observed MR was consistent with previous studies reaching a mean grade of 3.17±0.75 [13]. For the simulated conditions, MR was quantified by direct measurement using an electromagnetic flow probe. The mean *in vitro* mitral regurgitation fraction was found to reach 46±6 % and mean grade of 3+. In comparison to the chronic IMR animals, *in vitro* MR jets were observed to be asymmetric and originate from the tethered A3-P3 leaflets.

Comparison of Anterior Leaflet Mechanics

For control conditions, no significant differences were observed in the A2 leaflet strain between the control animals and simulated conditions in the radial (21±14 % vs. 32±18 %, p=.230) and circumferential (6±10 % vs. 11±7 %, p=.364) directions. Similarly, no significant differences were observed between the chronic IMR animals and simulated IMR conditions and in the radial (21±11 % vs. 34±18 %, p=.151) and circumferential (7±9 % vs. 9±7 %, p=.586) directions respectively. To determine if leaflet strain increases from a control to chronic IMR valve geometry, radial and circumferential strains were compared between the simulated conditions. In comparison to the control condition, results revealed a significant increase in radial (p=.028) and circumferential (p=.028) strains.

In addition to the peak measured values, the peak rate change of these strains (d(LVP)/dt) were determined during Isovolumetric contraction and compared between animal and simulation groups. Since these values are largely a function of the rate at which LVP increases, all d(LVP)/dt values were normalized by d(LVP)/dt (table 3). Results revealed no significant differences between the control animals and simulated control conditions in the radial (p=.873) and circumferential (p=.109) directions respectively. Similar results were observed between the chronic IMR animals in the radial (p=.631) and circumferential (p=.200) directions. To determine if leaflet strain rate increases from a control to chronic IMR valve geometry, radial and circumferential strain rates were compared between the simulated conditions. In comparison to the control condition, results revealed a significant increase in the normalized radial (p=.005) and circumferential (p=.018) strain rates.

Comment

Simulated changes in systolic MV geometry from control to chronic IMR were modeled within the GTLHS. With a chronic IMR MV geometry, significant decreases in coaptation length and significant increases in coaptation depth and tenting area were observed as clinically described [1-4]. These changes in leaflet coaptation were accompanied with MR jets of a magnitude similar to that observed in the ovine subjects In comparison to the simulated controls, a chronic IMR MV geometry resulted in significantly increasing both radial and circumferential anterior leaflet strains. This can be explained in that the IMR geometry increases the leaflet area exposed to the transmitral pressure resulting in a greater force and stretch within the tissue.

The annular MV geometric changes and MR observed within our animals are in excellent agreement with previous studies [13,14,24,25]. Since the coronary anatomy varies very little between sheep and they do not form collateral vessels, these sheep provide a reliable and repeatable model of chronic IMR [24]. Due to the precise control that's allowed by the simulator's components, the simulated annular dilatation and PM displacement is also very repeatable. During valve selection, great care was given to selecting valves of similar size to that in-vivo. While similar in size, the number of chordae per valve likely differed as did their geometric insertions to the PMs and leaflets. Even with this variability, the standard deviations found in the in-vitro MR fractions, coaptation characteristics, and strain was improved in comparison to previous studies [12,15,26,27].

Given the consistency of both models, the authors believe that demonstrating negative results with larger sample size would still not supersede or overcome the limitations of the in-vitro simulator. For these reasons, we believe the negative results reported herein are meaningful and highlights the unique ability of the simulator to mimic the systolic valvular distortions, coaptation, and anterior leaflet strain of a chronic IMR ovine model. These results additionally demonstrate the repeatability of the simulator and its ability to detect small differences between experimental conditions that can be difficult in animal or human studies.

For type IIIb dysfunctions, the ultimate goals are to cease MR and promote reverse LV remodeling [1-2]. The effectiveness of IMR repairs is dependent on the repair's ability to compensate for distended LV by restoring coaptation and ceasing MR during systolic closure [3-5]. For these reasons, the ultimate goal of our simulator is to mimic the systolic closure of the leaflets. And moreover, understand how to improve it. Hence, the ultimate goal of our simulator is to mimic the systolic closure of the leaflets and provide a platform to investigate how to improve it in repair conditions.

Provided the advantages of the described simulator, several limitations are associated with both the apparatus and the methodologies used in this study. The described mitral valve

simulator can recreate the systolic geometric configuration of the mitral valve but at current does not incorporate the intricate mechanics associated with valvular-ventricular interaction. Its inclusion would likely increase the accuracy of mimicking the dynamic *in vivo* valve function whose effects should be isolated in future studies. While at current the model can focus on the geometry of the annulus, leaflets, and PMs; evaluating repairs that directly affect the ventricle will require appropriate in vivo geometric boundary conditions.

In this study, the comparison of our simulated results is limited to an extensively studied inferior IMR ovine model and does not emulate the valvular distortion and function that may be seen in other etiologies. The IMR ovine model's resulting valvular geometry are likely dependent on infarct size and may change with a lesser or greater degree of myocardial infarction. The evaluation of leaflet coaptation was limited to the A2-P2 annular plane as the ability to quantify coaptation along the A3-P3 plane was limited due to the thin ill-coapting leaflets. In future studies, a broader spectrum of IMR valvular geometries (i.e. from more diffuse coronary disease or anterolateral infarction) should be simulated with similarities assessed between the *in vitro* and *in vivo* models. Dynamic leaflet motion within the simulator should additionally be evaluated.

In our studied animals, implantation of the miniature sonomicrometry transducers to the anterior leaflet likely influenced the local deformation of the anterior leaflet and could be improved with the use of radioopaque markers. For the computation of A2 leaflet strain, the number of transducers that could be localized to the ovine anterior leaflet was limited to 5 whereas in the GTLHS strain was computed with 9. While statistically significant differences between the measured parameters were not observed, we believe the differences in the magnitudes between each metric are representative of that which may be observed with larger sample size. Combined, these limitations must be assessed in coordination with the results of future studies that use the tested IMR valve geometry as a platform to evaluate MV repairs.

Our findings in this study demonstrate the ability of an in vitro simulator to mimic A2-P2 leaflet coaptation, anterior leaflet strain, and MR characteristics of healthy and chronic IMR ovine animals at peak systole. These results provide a foundation to evaluate the effect of IMR MV geometry on the effectiveness of current and future IMR repairs. A study is currently underway to examine the compensatory limits of undersized mitral annuloplasty and the effectiveness of ventricular based techniques in restoring coaptation. Upon additional investigation, these findings should provide key insight to the effect of MV geometry on repair effectiveness and contribute to our clinical understanding of the geometric based mechanisms that restore valvular competence.

Acknowledgments

This study was supported by a research grant awarded from the National Institute of Health (R01 HL090661-02) and from the National Heart and Lung Institute (HL063954, HL073021, HL103723, and HL108330). Robert Gorman and Joseph Gorman were supported by individual Established Investigator Awards from the American Heart Association.

References

1. Braun J, van de Veire NR, Klautz RJM, et al. Restrictive mitral annuloplasty cures ischemic mitral regurgitation and heart failure. Ann Thorac Surg. 2008; 85:430–437. [PubMed: 18222238]
2. Geidel S, Lass M, Schneider C, et al. Downsizing of the mitral valve and coronary revascularization in severe ischemic mitral regurgitation results in reverse left ventricular and left atrial remodeling. Eur J Cardiothorac Surg. 2005; 27:1011–1016. [PubMed: 15896610]

3. Kuwahara E, Otsuji Y, Iguro Y, et al. Mechanism of Recurrent/Persistent Ischemic/Functional Mitral Regurgitation in the Chronic Phase After Surgical Annuloplasty. Circulation. 2006; 114:I-229–I-534.
4. McGee EC, Gillinov AM, Blackstone EH, et al. Recurrent mitral regurgitation after annuloplasty for functional ischemic mitral regurgitation. J Thorac Cardiovac Surg. 2004; 128:916–924.
5. Braun J, Klautz RJM. Mitral valve surgery in low ejection fraction, severe ischemic mitral regurgitation patients: should we repair them all? Curr Opin Cardiol. 2012; 27:111–117. [PubMed: 22274572]
6. Ciarka A, Braun J, Delgado V, et al. Predictors of mitral regurgitation recurrence in patients with heart failure undergoing mitral valve annuloplasty. Am J Cardiol. 2010; 106:395–401. [PubMed: 20643253]
7. Mange J, Pibarot P, Dagenais F, Hachicha Z, Dumesnil JG, Sénéchal M. Preoperative posterior leaflet angle accurately predicts outcome after restrictive mitral annuloplasty for ischemic mitral regurgitation. Circulation. 2007; 115:782–791. [PubMed: 17283262]
8. Lee APW, Acker M, Kubo S, et al. Mechanisms of recurrent functional mitral regurgitation after mitral valve repair in nonischemic dilated cardiomyopathy: importance of distal anterior leaflet tethering. Circulation. 2009; 119:2606–2614. [PubMed: 19414639]
9. Buckley O, Di Carli M. Predicting benefit from revascularization in patients with ischemic heart failure: imaging of myocardial ischemia and viability. Circulation. 2011; 123:444–450. [PubMed: 21282521]
10. Vismara R, Pavesi A, Votta E, Taramasso M, Maisano F, Fiore GB. A pulsatile simulator for the in vitro analysis of the mitral valve with tri-axial papillary muscle displacement. Int J Artif Organs. 2011; 34:383–391. [PubMed: 21534249]
11. Bhattacharya S, He Z. Annulus tension of the prolapsed mitral valve correction by edge-to-edge repair. J Biomech. 2012; 45:562–568. [PubMed: 22153221]
12. He S, Jimenez JH, He Z, Yoganathan AP. Mitral Leaflet Geometry Perturbations with Papillary Muscle Displacement and Annular Dilation: an In-Vitro Study of Ischemic Mitral Regurgitation. J of Heart Valv Dis. 2003; 12:300–307.
13. Gorman JH III, Gorman RC, Jackson BM, Enomoto Y, St John-Sutton MG, Edmunds LH Jr. Annuloplasty ring selection for chronic ischemic mitral regurgitation: lessons from the ovine model. Ann Thorac Surg. 2003; 761556:1563.
14. Robb JD, Minakawa M, Koomalsingh KJ, et al. Posterior leaflet augmentation improves leaflet tethering in repair of ischemic mitral regurgitation. Euro J Cardio-thorac Surg. 2011; 40:1501–1507.
15. He Z, Ritchie J, Grashow JS, Sacks MS, Yoganathan AP. In Vitro Dynamic Strain Behavior of the Mitral Valve Posterior Leaflet. J Biomech Eng. 2005; 127:504–511. [PubMed: 16060357]
16. Padala M, Sacks MS, Liou SW, Balachandran K, He Z, Yogantahn AP. Mechanics of the mitral valve strut chordae insertion region. J Biomech Eng. 2010; 132:081004. [PubMed: 20670053]
17. Rabbah JP, Siefert AW, Spinner EM, Saikrishnan N, Yoganathan AP. Peak Mechanical Loads Induced in the in-vitro edge-to-edge repair of posterior leaflet flail. Ann Thorac Surg. 2012; 94:1445–1452.
18. Nielsen SL, Nygaard H, Fontaine AA, et al. Chordal force distribution determines systolic mitral leaflet configuration and severity of functional mitral regurgitation. J Amer Coll of Cardiol. 1999; 33:843–853. [PubMed: 10080490]
19. Jimenez JH, Soerensen DD, He Z, et al. Effects of a saddle shaped annulus on mitral valve function and chordal force distribution: an in vitro study. Ann Biomed Eng. 2003; 31:1171–1181. [PubMed: 14649491]
20. Sacks MS, Enomoto Y, Graybill JR, et al. In vivo dynamic deformation of the mitral valve anterior leaflet. Ann Thorac Surg. 2006; 82:1369–1378. [PubMed: 16996935]
21. Tibayan FA, Rodriguez F, Zasio MK, et al. Geometric distortions of the mitral valvular-ventricular complex in chronic ischemic mitral regurgitation. Circulation. 2003; 108:II-116–II-121. [PubMed: 12970219]
22. Rausch MK, Tibayan FA, Miller DC, Kuhl E. Evidence of adaptive mitral leaflet growth. J Mech Behavior Biomed Materials. 201210.1016/j.jmbbm.2012.07.001

23. Dal-Bianco JP, Aikawa E, Bischoff J, et al. Active adaptation of the tethered mitral valve: insights into a compensatory mechanism for functional mitral regurgitation. Circulation. 2009; 120:334–342. [PubMed: 19597052]

24. Llaneras MR, Nance ML, Streicher JT, et al. Large Animal Model of Ischemic Mitral Regurgitation. Ann Thorac Surg. 1994; 57:432–439. [PubMed: 8311608]

25. Gorman JH, Jackson BM, Enomoto Y, Gorman RC. The effect of regional ischemia on mitral valve annular saddle shape. Ann Thorac Surg. 2004; 77:544–548. [PubMed: 14759435]

26. Nielsen SL, Nygaard H, Mandrup L, et al. Mechanism of incomplete mitral leaflet coaptation-interaction of chordal restraint and chages in mitral leaflet coaptation geometry. Insight from in vitro validation of the premise of force equilibrium. J Biomech Eng. 2002; 124:596–608. [PubMed: 12405603]

27. He, Shengqui; Lemmon, JD.; Weston, MW.; Jensen, MO.; Levine, RA.; Yoganathan, AP. Mitral valve compensation for annular dilatation: In vitro study into the mechanisms of functional mitral regurgitation with an adjustable annulus model. J Heart Valve Dis. 1999; 8:294–302. [PubMed: 10399664]

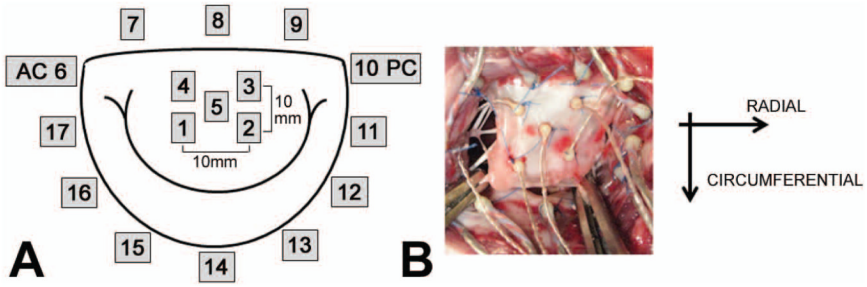

Figure 1.

A: Geometric map of sonomicrometry crystals localized to the A2 anterior leaflet and mitral annulus; AC: Anterior Commissure, PC: Posterior Commissure; B: in-vivo image of crystals localized to the mitral annulus and anterior leaflet with directions of strain shown.

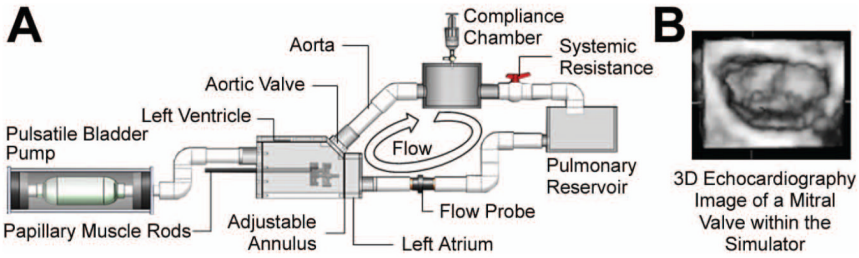

Figure 2.

A: Schematic of the mitral valve simulator with components identified; B: Atrial echocardiographic image of mitral valve closure during peak systole within the simulator.

Table 1

Baseline characteristics of the ovine subjects

	Weight (kg)	Heart Rate [beats/min]	Peak LVP [mmHg]	dLVP/dt [mmHg]	Infarcted LV Endocardium (%)	Anterior Leaflet Height [cm]	Mitral Annular Area [cm^2]
Control	38 ± 2	98 ± 15	103 ± 6	1842 ± 493	0	1.8 ± 0.1	6.4 ± 1.2
Chronic IMR	39 ± 2	100 ± 13	101 ± 8	1592 ± 490	18.5 ± 1.6	1.9 ± 0.1	10.4 ± 2.2

Table 2

A2-P2 coaptation characteristics between the animal and simulated valves

		Coaptation Length [mm]	Coaptation Depth [mm]	Tenting Area [cm^2]
Control	**Animal**	4.4 ± 0.4	1.8 ± 0.2	0.23 ± 0.07
	Simulator	4.0 ± 0.4	2.1 ± 0.3	0.16 ± 0.05
Chronic IMR	**Animal**	3.2 ± 0.3	2.4 ± 0.8	0.27 ± 0.13
	Simulator	3.1 ± 0.6 *	2.8 ± 1.0 *	0.31 ± 0.13 *

*denotes a $p<0.05$ significant difference between the chronic IMR and control simulated conditions.

Table 3

Normalized strain rate

		Normalized Strain Rate [mm/(mm·mmHg]·100%	
		Radial	**Circumferential**
Control	**Animal**	0.24 ± 0.21	0.20 ± 0.13
	Simulator	0.23 ± 0.05	0.11 ± 0.07
Chronic IMR	**Animal**	0.30 ± 0.18	0.20 ± 0.13
	Simulator	0.52 ± 0.14 †	0.16 ± 0.06 *

* denotes a p<0.05 and

† denotes a p<.01 significant difference between the chronic IMR and control simulated conditions.